Desalination 253 (2010) 16–21

Contents lists available at ScienceDirect

Desalination

journal homepage: www.elsevier.com/locate/desal

Effect of flow deflector on the flux improvement in direct contact membrane distillation

Chu-Lien Liu [a], Yu-Feng Chen [b], Wen-Junn Sheu [a], Chi-Chuan Wang [c,*]

[a] Department of Power Mechanical Engineering, National Tsing Hua University, Hsinchu 300, Taiwan
[b] Energy & Environment Research Laboratories, Industrial Technology Research Institute, Hsinchu 310, Taiwan
[c] Department of Mechanical Engineering, National Chiao Tung University, Hsinchu 300, Taiwan

ARTICLE INFO

Article history:
Received 3 September 2009
Received in revised form 19 November 2009
Accepted 27 November 2009
Available online 3 January 2010

Keywords:
Membrane distillation
Heat transfer coefficient
Flow deflector

ABSTRACT

This study experimentally investigated the influence of flow deflector on the performance of direct contact membrane distillation. A total of seven modules, including a smooth membrane module and six flow deflector modules were fabricated and tested. Effects of the number of flow deflector, deflector height, and the placement of deflectors are examined. The smooth module reveals a comparatively abrupt change of water flux when the inlet velocity is around 0.25 m s^{-1}, and a plateau is seen for the water flux ratio vs. the Reynolds number for modules containing flow deflectors. Depending on the arrangement of flow deflectors, the maxima occur at a Reynolds number of 500 for D1 and 650 for the others. The plateau for module having more flow deflectors has shifted toward a lower Reynolds number while the pressure drop ratio does not reveal such a plateau. For the same pumping power, the test results show that the water flux for smooth module are smaller than that of all flow deflector modules, and it is applicable to all temperatures. It is also found that modules with more deflectors become more and more competitive at a higher feed temperature but are less effective when the velocity is high.

1. Introduction

Membrane distillation (MD) is a hybrid of thermal distillation and membrane processes. It features a thermally driven process via a microporous membrane separating the warm and cold solutions. The vapor pressure difference is generated through the non-isothermal process between feed side and permeate side, thereby vapor molecules will transport from the warm feed side into the hydrophobic membrane pores provided the vapor pressure is being established. Fig. 1 is a schematic showing the typical MD membrane and its heat/mass transport mechanisms. Evaporation occurs at the warm feed side, yet the vapor molecules migrate across the non-wetted pores to condense at the permeate side. Consider a plate configuration, the overall heat transfer process is given as [1]:

$$q = \frac{T_f - T_p}{\left(\frac{1}{h_f} + \frac{1}{\frac{k_m}{\delta} + \frac{J\lambda}{\Delta T_m}} + \frac{1}{h_p}\right)} \quad (1)$$

From Eq. (1), three resistances prevail for the heat transport from warm feed side to cold permeate side, namely the convective resistance of feed side ($1/h_f$) and permeate side ($1/h_p$) and the membrane resistance ($\frac{1}{\frac{k_m}{\delta} + \frac{J\lambda}{\Delta T_m}}$). For direct contact membrane distillation, normally the feed side resistance is larger than that of the permeate side [2,3], yet it plays a crucial role in the overall heat transport process of MD. This is especially critical for an elevated feed side temperature since the thermal process is controlled by the feed side. In this regard, some passive or active methods to reduce feed side resistance offer promising aspects for significant energy saving. Fane and Chang [1] had summarized techniques to enhance performance of membrane process using both passive and active methods. Passive methods are more convenient for no additional power is required. Commonly passive enhancements take the forms like Net-type spacer (Da Costa and Jane [4]), helical inserts (Gupta et al. [5]), and corrugated membrane (Bertram et al. [6]). In opposition to the forgoing passive augmentations, Sobey [7] found that by imposing an oscillatory motion on a single flow deflector in a membrane channel could produce many vortices called "vortex wave". Millward et al. [8] then showed that by adding narrowly spaced flow deflectors to the membrane channel augments the flux by a factor of 3.5 relative to a plain channel at a Reynolds number of 123. More importantly, the deflectors offers very small rise of pressure drop penalty. Their results inspire the present study to examine the flow deflectors on the performance of direct contact membrane distillation. The objective of this study aims at the effect of passive flow deflectors alone (without imposing any oscillatory motion) on the overall performance. A variety of geometric arrangements, including number of

* Corresponding author. D100 ERL/ITRI, Bldg. 64, 195~6 Section 4, Chung Hsing Rd., Chutung, 310, Hsinchu, Taiwan. Tel.: +886 3 5916294; fax: +886 3 5820250.
E-mail address: ccwang@itri.org.tw (C.-C. Wang).

0011-9164/$ – see front matter © 2009 Elsevier B.V. All rights reserved.
doi:10.1016/j.desal.2009.11.042

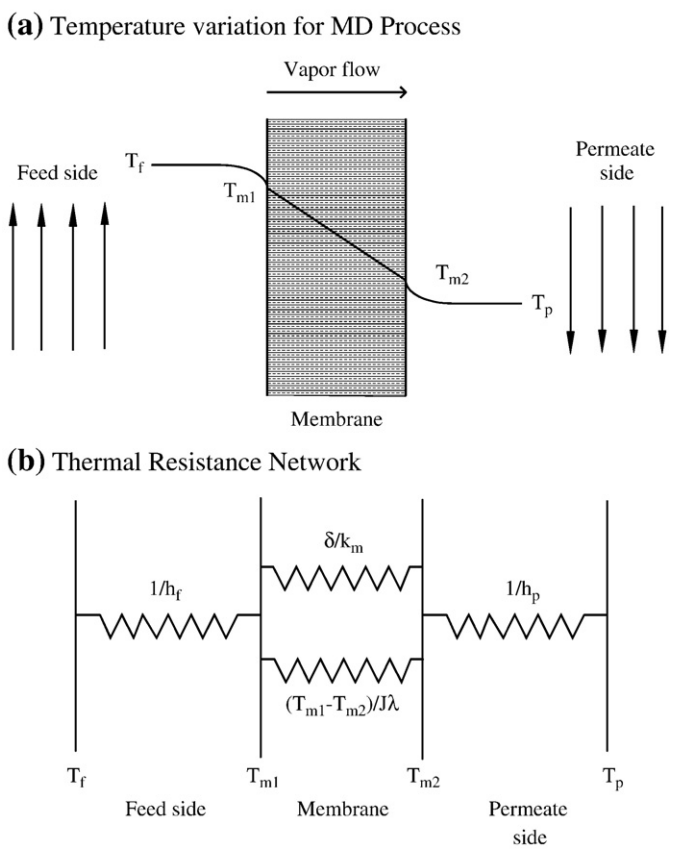

Fig. 1. Schematic showing the temperature variation for membrane distillation across and the associated thermal resistance network.

deflector, deflector height, and deflector position, will be investigated in this study.

2. Experimental setup

A flat sheet membrane module with the membrane being Millipore FGLP14250 (PTFE) having an average pore size of 220 nm, a porosity of 0.7, a membrane thickness of 61 μm, and a thermal conductivity of 0.28 $Wm^{-1}K^{-1}$ was used in this study. The membrane module was made from acrylic with membrane being placed between feed and permeate sides, and the feed side and the permeate side each contains four identical flow channels with the dimension of each channel being 4 mm wide, 100 mm long, and 1.0 mm high. A total of seven membrane modules, including a smooth channel and six flow deflectors, are fabricated. Their detailed dimension and arrangements of the deflector are shown in Fig. 2(a) and (b) is a typical photo of the test module (*D*2). The designations of *D*1 and *D*5 channels represent full of deflectors with deflector heights of 0.8 and 0.4 mm, respectively. *D*2, *D*3, and *D*6 denote half-filled deflectors with the flow deflectors being placed at the entrance part for *D*2 whereas the flow deflectors for *D*6 and *D*3 are located at the second half portion. *D*4 is a quartered filled design with deflector height of 0.8 mm. In all experiments, the membrane modules are placed horizontally. Distilled water was used as the working fluid in both feed and permeate sides. Fig. 3 is a diagram of the test apparatus. Volumetric pumps were used to deliver distilled water across the test section. Pressure and temperature on the inlet and outlet streams of the membrane module on both warm and cold sides were measured using manometers and thermo-resistance RTD (Pt100). The RTDs were pre-calibrated with an accuracy of 0.1 °C. The pressure drops at the feed side are measured by a YOKOGAWA

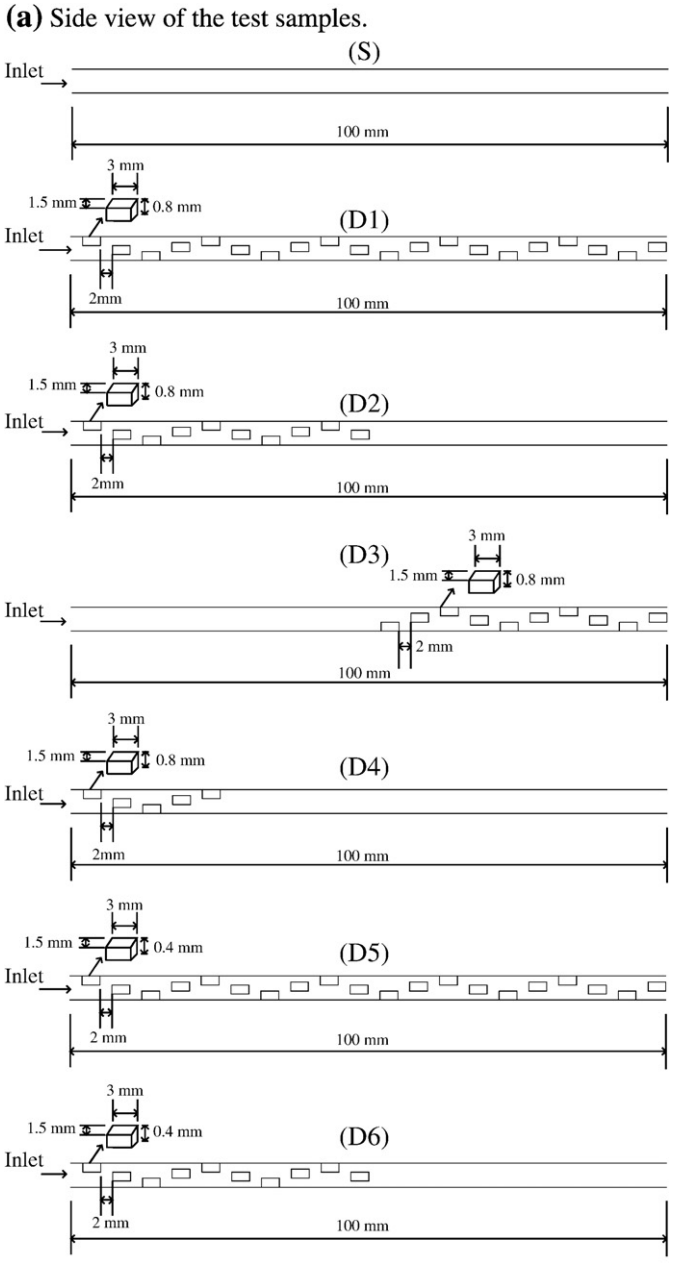

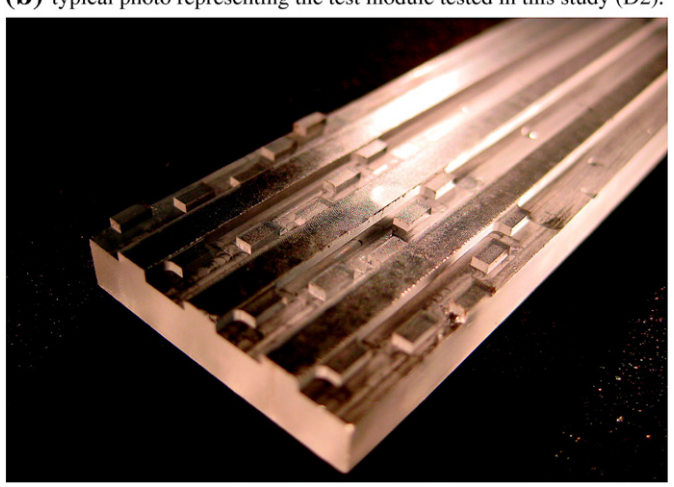

Fig. 2. Schematic of the test channel with and without flow deflectors.

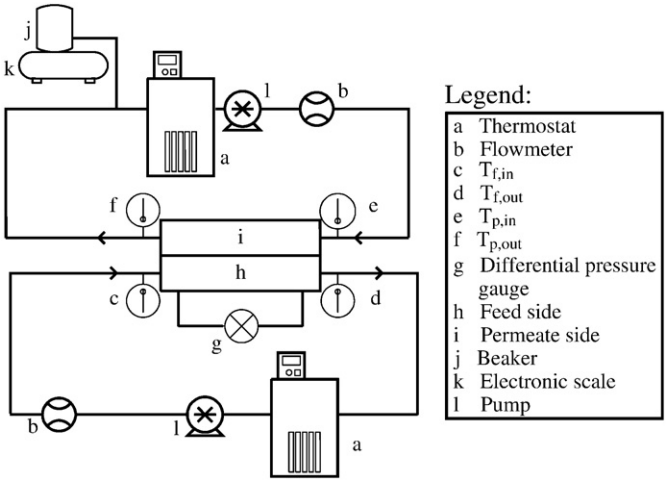

Fig. 3. Schematic of the test apparatus.

EJ110 differential pressure transducer having an adjustable span of 1300 to 13,000 Pa. Resolution of this pressure differential transducer is 0.3% of the measurements. Tests were performed at a fixed permeate side temperature of 25.8 °C while the average feed side temperature are maintained at three temperatures (41.6 °C, 51.6 °C, and 61.6 °C, respectively). Steady state water flux and pressure drop across the membrane are recorded for various flow rates.

3. Results and discussion

Fig. 4 is a typical result for flux vs. inlet velocity subject to the influence of feed side temperature. Note that the average permeate side temperature is maintained at 25.8 °C. As seen in Fig. 4, the flux is increased with the rise of inlet velocity. Apparently, the influence of inlet velocity becomes more evident at a higher feed temperature. This is because the membrane resistance plays the essential role in the whole thermal resistance at a lower feed temperature. In this sense, the increase of feed side velocity offers very small augmentation of the water flux. In fact, for an inlet temperature of 41.6 °C, a seven-fold increase of inlet velocity (0.6–4.2 m s^{-1}) raises only approximately 6% of flux. In the meantime, when the average feed side temperature is elevated to 61.6 °C, the corresponding increase of flux subject to velocity change is as high as 46%. In opposition to the water flux, the pressure drops increase substantially with the inlet velocity but decrease moderately with the feed temperature. This is somehow expected due to the decrease of viscosity at elevated temperatures.

For the water flux subject to the various deflector arrangements, a typical result for the full deflector is shown in Fig. 5. The general trend looks similar to that of smooth channel, the flux is increased with the inlet velocity or with temperature, yet the influence of feed velocity becomes quite pronounced at an elevated temperature. However, there is a distinction amid smooth and deflector channels. As shown in Fig. 4, the slopes of the flux for the smooth channel are roughly classified into two regions. At a lower flow velocity regime (V_f<0.2 m s^{-1}) the flux increases comparatively slowly with the inlet flow velocity while at a higher inlet velocity regime (V_f>0.25 m s^{-1}) the water flux increases more rapidly with the inlet velocity. In short, the smooth channel reveals a comparatively abrupt change in flux vs. velocity. By contrast, the water flux vs. inlet velocity having a deflector design ($D1$) does not reveal this unusual characteristic. The water flux increases relatively smoothly with the rising inlet velocity as shown in Fig. 5. For further illustration of this phenomenon, one can examine the corresponding reciprocal of the inverse Graetz number x^+, which is defined as

$$x^+ = \frac{L/D_h}{Re_{D_h} Pr,} \tag{2}$$

where L is the streamwise duct length, Pr is the Prandtl number, and $Re_{D_h}\left(=\frac{\rho V D_h}{\mu}\right)$ is the Reynolds number based on hydraulic diameter. The flow may be considered fully developed when x^+>0.05 [9] which corresponds to a velocity being less than 0.2 m s^{-1} for the present study. Hence it suggests the major portion of the test section falls within fully developed region when the inlet velocity is low, leading to a negligible improvement in heat transfer. As a consequence, the smooth channel shows very small augmentation at this low velocity regime. In the meantime, a detectable rise in flux with inlet velocity is observed at a higher velocity regime. This is because the flow in the channel is in developing flow whose heat transfer performance is more related to the flow velocity. As a consequence, both fully developed and developing characteristic prevails in the smooth channel, leading to an abrupt change of slope of water flux. In the meantime, the channel with flow deflector does not exhibit this kind

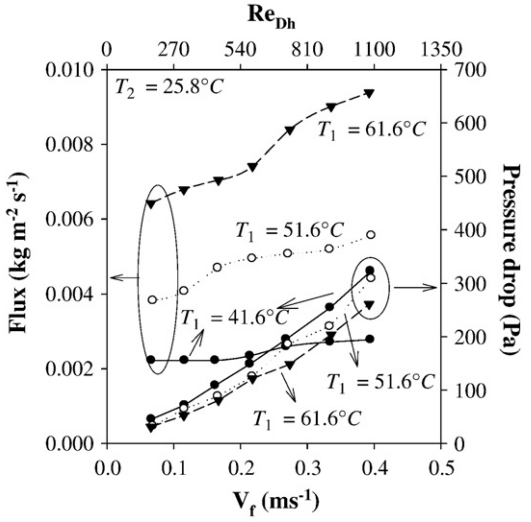

Fig. 4. Water flux and pressure drop vs. feed side velocity subject to feed side temperature for smooth channel module.

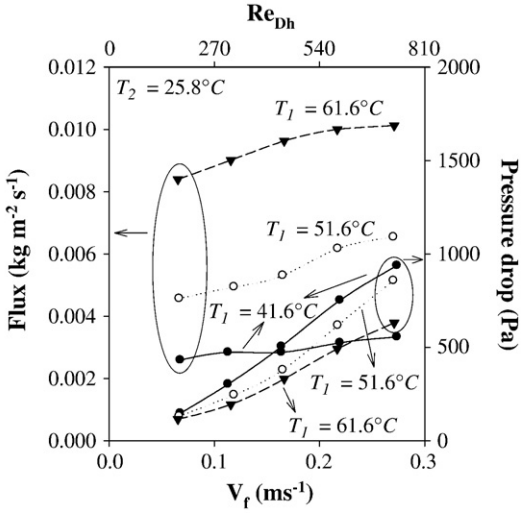

Fig. 5. Water flux and pressure drop vs. feed side velocity subject to feed side temperature for full flow deflector (D1) module.

of phenomenon. This is because the presence of flow deflector has completely eliminated the "fully developed regime" even at a very low flow velocity. Therefore the water flux rises steadily against the velocity. In fact all the flow deflector modules share the same feature (no abrupt change in water flux).

For further evaluation of the performance of flow deflector, the performance is termed as flux augmentation ratio J_D/J_S and pressure drop penalty ratio $\Delta P_D/\Delta P_S$ vs. the Reynolds number. Where the subscript D represents with flow deflector and S denotes smooth channel. The corresponding results for $T_f = 61.6$ °C and $T_p = 25.8$ °C with the six flow deflectors are shown in Fig. 6. As seen in the figure, the channel with high flow deflector ($D1$) has the highest flux augmentation of about 36% and a considerable rise of pressure drop penalty (over 4.2 times), followed by the half-filled flow deflectors ($D2$/$D3$), quartered-fill flow deflector ($D4$), and the medium height flow deflectors ($D5$/$D6$). It is interesting to know that the ratio of J_D/J_S peaks at a Reynolds number of 500 for $D1$ and 650 for the others while the pressure drop ratio does not clearly show this trend and in fact they steadily rise with the Reynolds number (except $D2$ where a slight undershoot is seen when Re surpasses 800). In the meantime, the plateau of water flux for those containing more flow deflectors are slightly shifted toward a lower Reynolds number. The results suggest that flow deflectors become less and less effective when the Reynolds number is above certain threshold value. In the present study, depending on the number of deflector and deflector height, the value is around 500 for $D1$ and around 650 for others. The earlier peak in water flux for more deflector module shown in Fig. 6 is associated with the general understanding of laminar/turbulent flow. For a turbulent boundary layer flow, the thermal resistance falls within a very short distance close to the wall, hence roughness can provide an effective augmentation of heat transfer without appreciable pressure drop penalty (Webb and Kim [10]). On the other hand, the dominant thermal resistance for the laminar flow is not limited to a thin boundary layer adjacent to the flow, thereby devices like the present flow deflectors that mix the gross flow are quite effective when the flow is laminar. In this study, the presence of the flow deflector may alter the flow and result in a much earlier turbulent transition toward a very lower Reynolds number, and accordingly it results in a plateau phenomenon subject to a change of the flow pattern. The phenomenon can be further substantiated by the shift of Reynolds number for surfaces containing more flow deflectors for they provide better mixing and are prone to flow transition. Therefore one can see the most complex flow deflector ($D1$) peaks at the lowest Reynolds number around 500. Results shown in Fig. 6 also imply that it is more effective to place the flow deflector in the entrance region ($D2$) rather than in the developed region ($D3$). This is because better mixing causes by the flow deflectors at the entrance region prevails alongside the downstream smooth region. By contrast, placing the flow deflectors at the developed region ($D3$) is less effective for there is less downstream flow region. Notice that the idea of using the half-filled flow deflector ($D2$/$D3$) is to reduce the pressure drop penalty. The quartered-fill flow deflector ($D4$) with a deflector height of 0.8 mm has an equal performance with the full flow deflector ($D5$) having a medium deflector height of 0.4 mm.

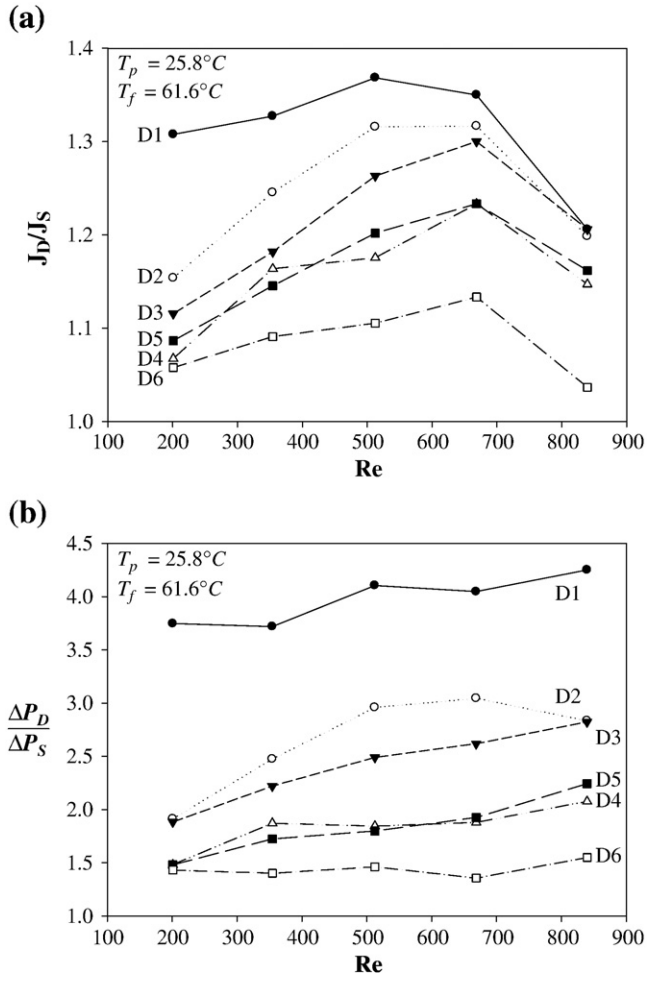

Fig. 6. Ratios of (a) water flux; and (b) pressure drop vs. Reynolds number for all flow deflector modules at an average feed temperature of 61.6 °C.

Based on the forgoing discussion, normally more flow deflectors engender higher water flux improvements but they also accompany with higher pressure drop penalty. For further comparison of the relative performance among the present flow deflectors, Fig. 7 presents the water flux vs. supplied pumping power ($V\Delta P$) for all the flow deflectors. For the same pumping power, the test results show that the water flux for smooth channel is smaller than that of all flow deflector modules, and it is applicable to all feed temperatures. On the other hand, modules with more deflectors become more and more competitive at an elevated feed temperature. This is in fact related to the pressure drop characteristics. As shown in Fig. 5, influence of temperature on pressure drops for more complex flow deflector is comparatively conspicuous than that for the smooth channel. In the meantime, it is interesting to know that the water flux for module with more flow deflectors shows an earlier level off than modules with the less flow deflector. For instance, at a feed temperature of 61.6 °C, the increasing trend of water flux vs. pumping power becomes relatively small for $D1$ when the pumping power is above 0.0004 W while the rest of the modules, especially for those with less deflector design or with smooth surface still show slowly an increase trend of water flux vs. pumping power. With a lower feed temperature, the level of phenomenon for $D1$ becomes obscure and is prolonged to a much larger pumping power. The results are in line with the forgoing discussion that more flow deflectors are more effective in the lower Reynolds number region.

4. Conclusion

The present study examines the influence of flow deflector on the performance of direct contact membrane distillation. A total of seven modules are made and tested, including a smooth membrane module and six flow deflector modules. A variety of geometric influences of flow deflectors have been studied, including the number of flow deflectors, deflector height, and the placement of deflectors. Based on the present experimental findings, the following results are concluded:

(1) The water flux is increased with inlet flow velocity or with the feed temperature for all the membrane modules. However, in

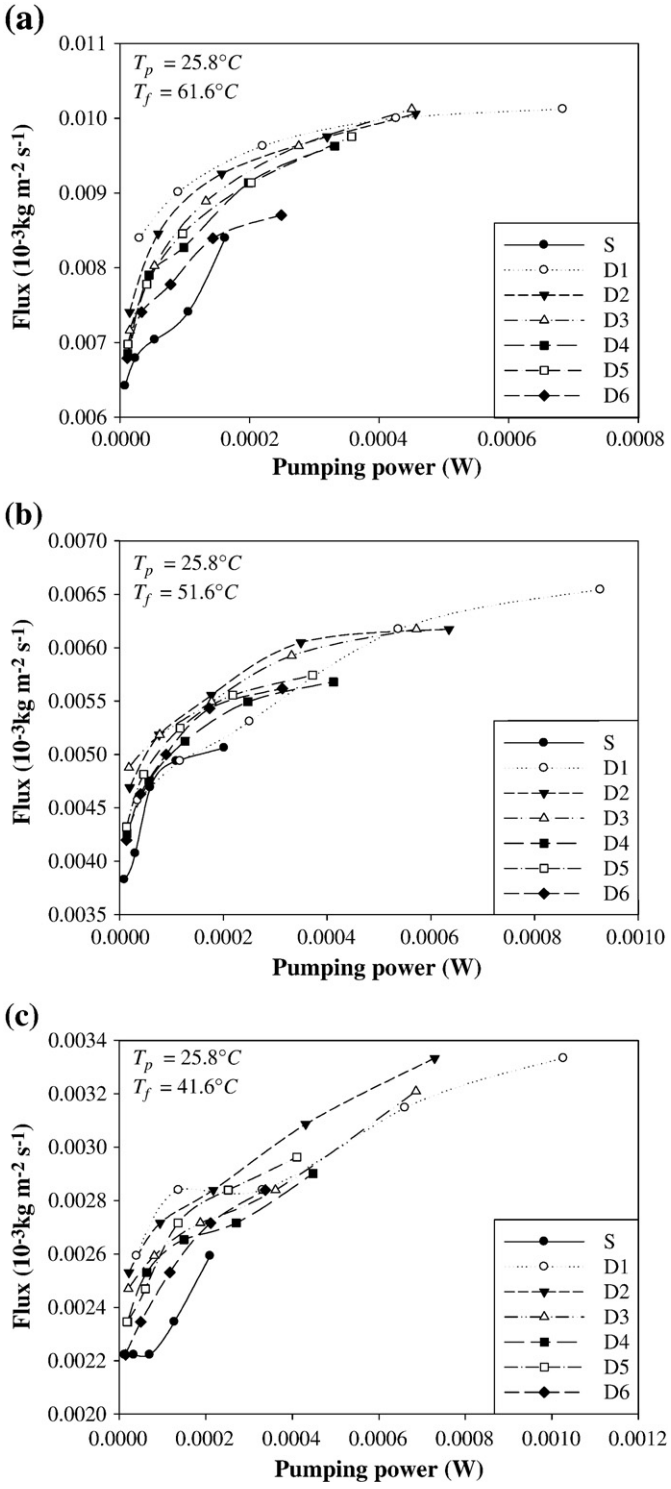

Fig. 7. Water flux vs. pumping power for all modules at (a) T_f = 61.6 °C; (b) T_f = 51.6 °C; and (c) T_f = 41.6 °C.

comparison with the smooth and deflector modules, it appears that the smooth modules reveal a comparatively abrupt change in water flux when V_f is close to 0.25 m s^{-1}. This is associated with the fully developed/developing characteristics of the smooth channel.

(2) Normally, a much higher water flux is achieved with the more compact module but it also accompanies with a much higher pressure drop penalty. The maximum enhancement of water flux is about 36% for the most compact module, yet a 4.2 times increase of pressure drop is encountered.

(3) A plateau of the water flux ratio vs. the Reynolds number is seen for those flow deflector modules. Depending on the arrangement of flow deflectors, the maxima occur at a Reynolds number of 500 for *D*1 and 650 for the others. The plateau has shifted toward a lower Reynolds number for the module having more flow deflectors. In the meanwhile, the pressure drop ratio does not reveal such maximum phenomenon.

(4) For the same pumping power, the test results show that the water flux for smooth channel module is smaller than that of all flow deflector modules, and it is applicable to all temperatures. On the other hand, modules with more deflectors become more and more competitive at a higher feed temperature but are less effective when the velocity is high.

Nomenclature

A	surface area (m^2)
D_h	hydraulic diameter (m)
h	heat transfer coefficient (W m^{-2} K^{-1})
J	Water flux (kg m^2 s^{-1})
k	thermal conductivity, (W m^{-1} K^{-1})
L	channel length, (m)
$\dot{V}$	volumetric flow rate (m^3 s^{-1})
Nu	Nusselt number
Pr	Prandtl number
q	heat flux (W m^{-2})
$\dot{Q}$	heat transfer rate (W)
T	temperature (°C)
V	velocity (m s^{-1})
x^+	inverse Graetz number, defined in Eq. (8)

Greek symbols

ε	porosity
δ	membrane thickness (m)
ΔT_m	temperature difference across membrane (K)
ΔP	pressure drop across membrane module (Pa)
λ	heat of evaporation (kJ kg^{-1})
μ	dynamic viscosity (kg m^{-1} s^{-1})
ρ	density (kg m^{-3})

Subscripts

ave	average value
D	deflector module
f	feed side
g	gas phase
m	membrane
m1	membrane in contact with the feed side
m2	membrane in contact with the permeate side
p	permeate side
s	solid phase
S	smooth channel

Acknowledgements

This work was supported by the Energy Bureau and Department of Industrial Technology, both from Ministry of Economic Affairs, Taiwan.

References

[1] A.G. Fane, S. Chang, in: A.K. Pabby, S.S.H. Rizvi, A.M. Sastre (Eds.), Handbook of Membrane Separation, CRC Press, 2009, pp. 193–232.
[2] J. Phattaranawik, R. Jiraratananon, A.G. Fane, J. Membr. Sci. 212 (2003) 177–193.
[3] A.M. Alkaibi, N. Lior, J. Membr. Sci. 282 (2006) 362–369.
[4] A.R. Da Costa, A.G. Fane, Ind. Eng. Chem. Res. 33 (1994) 1845–1851.
[5] B.B. Gupta, J.A. Howell, D. Wu, R.W. Field, J. Membr. Sci. 102 (1995) 31–42.
[6] C.D. Bertram, M.R. Hoogland, H. Li, R.A. Odell, A.G. Fane, J. Membr. Sci. 84 (1993) 279–292.
[7] I.J. Sobey, J. Fluid Mech. 151 (1985) 395–426.
[8] H.R. Millward, B.J. Bellhouse, I.J. Sobey, Chem. Eng. J. Biochem. Eng. J. 62 (1995) 175–181.
[9] R.K. Shah, A.L. London, Laminar flow forced convection in ducts, Academic Press, 1978.
[10] R.L. Webb, N.H. Kim, Principles of enhanced heat transfer, 2nd edTaylor and Francis, 2005.